Design of Biosensor for Diagnosis of Biomolecules Using Surface Enhanced Raman Spectroscopy

B. Hasanshahi [a], S.J. Sayyedfattahi [a*]

[a] Department of Electrical and Electronic Enginering, Islamic Adad University, Tabriz Branch, Tabriz, Iran
*** Corresponding author email: s.sayyedfattahi@iaut.ac.ir**

Received: Jul. 28, 2021, Revised: Sep. 15, 2021, Accepted: Nov. 21, 2021, Available Online: Mar. 8, 2022
DOI: 10.30495/ijbbo.2021.686484

ABSTRACT— In recent years, surface enhanced Raman Spectroscopy (SERS) method have been applied in the area of biotechnology, nanotechnology and diagnostic issues. For that, nanoparticles have been arranged near the flat film structure. By doing so, it is found that the local field enhancement can be greatly improved. In this paper, using two type of nanoparticles namely Ag, Au, we have obtained a double resonance system structure. The process is carried out by the application of nanoparticles, Ag and Au with Ag as a grating coupler. The space and interspace of 3 nm and 5-20 nm for the two particles Au and Ag are considered, respectively. A double resonance system structure has been proposed and simulated with the LUMERICAL FDTD. Our result show that for nanoparticle-film coupling, the highest enhancement factor of ($\mathbf{10^{13}}$) can be obtained for Ag nanosphere and Ag-grating coupler. Finally the simulation results show that application of multiple couplings associated with Ag grating filed and tooth like binding of Ag grating coupling can be used to significantly improve the near-field enhancement.

KEYWORDS: nanoparticle, Raman spectroscopy, FDTD

I. INTRODUCTION

Surface enhanced Raman spectroscopy (SERS) is a powerful technique in detecting low concentration analyte in order to obtain specific information about physical and chemical characterization of analytes. One way to enhance the Raman intensity is due to the process of electromagnetic mechanisms that occurs because of an enhancement in the electric field strength, provided by the surface plasmons (1-7). When the incident light impinges upon the surface, conduction electrons at the surface begin to oscillating causing the amplification of the SERS signals strength. This is because of the concentration of the local EM fields in the near field of the nanogap hot spots. SERS signal are typically assumed to be proportional to the 4th power of the factor $\left|\frac{E_{Local}}{E_0}\right|$. We can define the SERS enhancement factor as $EF = I_{SERS} / < I_{RS} >$, where I_{SERS} is the SERS intensity and $< I_{RS} >$ is the conventional Raman intensity under the same conditions, averaged over all possible orientations of the probe. Because if the existing of two nano structure next to each other, hot spots are created, causing the amplification of the electric field strength, between two nanostructure (8-11). Considering the fact that "Plasmonic coupling" is the key factor in this process, the maximum SERS enhancement factor may be as high as 10^{11} (12). Of course the enhancement factor may be used to detect the SERS signals from a single molecule (13-14). It is worth to mention, the material structure, geometry and polarization of the incident laser beam can have effect on the enhancement factor. For example metallic structures are good for SERS, substrate due to their significant effect on the plasmonic resonance for the visible light spectrum. The geometry of structure, can also have a good effect on the surface plasmonic resonance. The role of polarization of plasmonic resonance due to laser beam should not be underestimated, because it has a positive effect on the SERS

hotspots (15-21). Today, the geometry of SERS substrate has taken much attention due to its ability to support strong plasmonic resonance. In particular, to achieve a smtrong local field enhancement, nanoparticles have been kept separate from a thin flat film in order to create a strong local filed enhancement (12). To investigate the plasmonic effect of this process, numerical analysis of the electromagnetic filed is needed. There are numerous method to do that for example, finite-difference time-domain (FDTD) (22), discrete dipole approximation method (23), and finite element analysis (24) to name a few. Among these, the most popular method is FDTD, where the light scattering from the particle is simulate. It should be noted that in the FDTD method we can obtain electric and magnetic fields at different locations in the time domain by numerically solving Maxwell equations (25).

In this paper, a double resonance system structure has been proposed and simulated by keeping in mind that metallic nanoparticles is located close to the metallic grating coupler. By doing so, the LUMERICAL FDTD has been used and with the calculation of electric filed distribution and enhancement factor. Our simulation results show the highest enhancement factor of 10^{13}as well as uniform distribution for the enhancement. Figure 1 shows the schematic diagram of double resonance coupling system under consideration. Where the biomolecules are located in the space between Ag-grating coupler and Ag-nanoparticle.

II. THEORETICAL MODELING AND FDTD SIMULATION

A. *Theoretical modeling*

Electromagnetic modeling was performed by application of Lumerical FDTD method. The model consisted of a three dimensional Ag nanosphere geometry (26) with dimensions $400 \times 400 \times 150$ nm and Au grating coupler with thicknesses of 1nm as a substrate. Slope of each took-like binding was considered 90° with the rate of each tooth height to the spacing in-between was chosen to be 0.5 incident light was taken to be normal to the surface of substrate, with polarization phase angle of zero degree. The range of the simulation was considered to be 5-50nm. A 1 nm global mesh was used; in order to improve accuracy, the mesh size was reduced in the gap region to 0.4 nm. The model was simulated with 200 points of 5 nm each with total interval of the simulation being (300-1300 nm). A 3 nm spacer with index of refraction (n) = 1 for initial calculation and n=1.37-1.52 for biomolecule (proteins) (27-30) was added. The surrounding boundaries were the perfectly matched layer. The simulation model is shown in fig 2.

B. *FDTD Simulation*

To investigate the surface enhanced Raman scattering behavior of metallic nanoparticle and metallic grating coupler, FDTD method was carried out to simulate electric and magnetic field intensity distribution. In order to build a model that consist of infinitive metallic nanoparticle and metallic coupler, we use periodic boundary. In this model, firstly, we use 2 type of nanosphere which are gold and silver with the radius 80nm, furthermore, silver grating coupler with 5 different spacer (25, 20, 15, 10, and 5) was simulated in order to calculate enhancement factor and intensity of electric field in which intensity of electric field is $\left|\frac{E_{Local}}{E_0}\right|$.

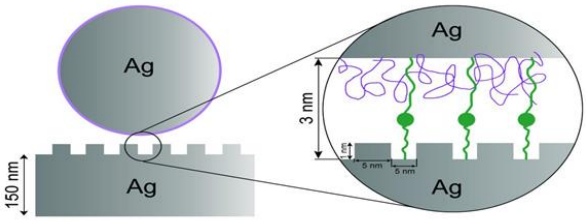

Fig. **1** SERS substrate schematic, a schematic of the Ag nanosphere as an example on an Ag grating coupler film.

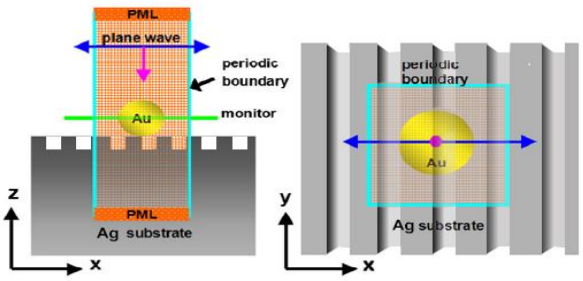

Fig. **2** Schematic representation of nanosphere coupling grating coupler system in the FDTD simulation.

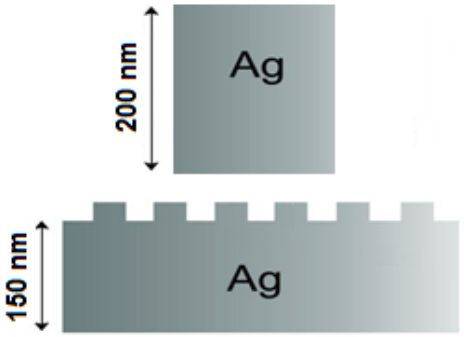

Fig. **3** Schematic representation of nanorod grating coupler system in the FDTD simulation.

RESULT AND DISCUSSION

The results of the simulation are listed in table 1.

Table **1** illustrate effect of 5 teeth spaces and 80 nm spheres on the a) enhancement factor b) field intensity.

a)

Nano sphere (80nm)	Enhancement factor				
	5nm	10nm	15nm	20nm	25nm
Ag	6.12×10^{13}	1.48×10^{11}	3.27×10^{10}	9.86×10^{8}	7.68×10^{8}
Au	5.18×10^{11}	3.28×10^{10}	1.02×10^{8}	8.35×10^{7}	7.23×10^{7}

b)

Nano sphere (80nm)	Field intensity				
	5nm	10nm	15nm	20nm	25nm
Ag	1.05×10^{7}	3.45×10^{6}	9.48×10^{5}	3.23×10^{4}	2.77×10^{4}
Au	9.16×10^{5}	1.18×10^{5}	1.02×10^{4}	8.35×10^{3}	7.23×10^{3}

As it can be seen, silver nanosphere coupling with subintervals of 5nm, has the largest enhancement factor. Also, at is clear that there exist an inverse relationship between electric field, enhancement factor and spacing with tooth like bindings. When the space between teeth of grating coupler increase, one of the resonance vanished so the enhancement factor and electric field decrease. As can be seen from the table 1, the absent of double resonance phenomena for the interval 15-25 nm is very clear.

Next, by considering gold and silver nanorod of 50nm radius Fig. 3 in each and the same grating couplers before we notice, the highest enhancement factor of $\mathbf{2.42\times10^{10}}$ for the nano silver rod. The results are shown in table 2

The effects of the incident laser beam polarization on the enhancement factor, has been investigated. By considering two types of polarization, that is P and S-polarization with the Ag grating coupler, as it be seen in the table 3, p-polarization has the largest enhancement factor, also the p-polarization has caused a considerable increase in the electric field intensity. Because P-polarization is efficiently coupled to the Plasmon resonance of the substrate.

Table **2** illustrate effect of 5 teeth spaces and 50 nm rods on the a) enhancement factor b) field intensity

a)

Nano rod (50nm)	Enhancement factor				
	5nm	10nm	15nm	20nm	25nm
Ag	6.12×10^{11}	3.49×10^{10}	3.27×10^{9}	9.86×10^{8}	7.68×10^{8}
Au	1.83×10^{11}	1.05×10^{10}	3.12×10^{9}	8.35×10^{8}	3.83×10^{8}

b)

Nano rod (50nm)	Field intensity				
	5nm	10nm	15nm	20nm	25nm
Ag	9.05×10^{5}	2.12×10^{5}	8.99×10^{5}	7.83×10^{4}	3.27×10^{4}
Au	8.36×10^{5}	1.01×10^{5}	5.35×10^{5}	4.12×10^{4}	2.83×10^{3}

Table **3** illustrate two type of polarization effect on the enhancement factor and field of Ag nanosphere and grating coupler system.

polarization	Enhancement factor	field intensity
P polarization	6.12×10^{13}	7.45×10^{6}
S polarization	2.42×10^{10}	1.53×10^{10}

The spatial electric field intensity ($|E/E_0|^2$) distribution is shown in Fig. 4. As we can see in the figure. 3 the field intensity is in the order of 10^6 which is in the spaces between grating coupler and nanosphere. Our theoretical results show the largest enhancement factor for Ag nanosphere considering Ag nano grating coupler.

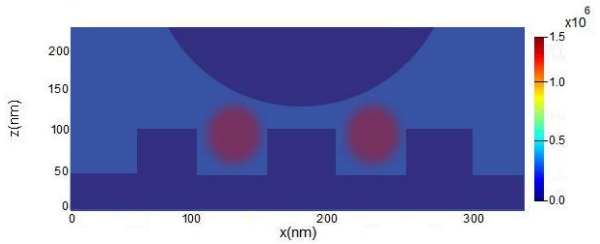

Fig. **4** illustrate electric field distribution ($|\boldsymbol{E/E_0}|^2$) around the Ag sphere and grating coupler in which the highest electric field is between of grating coupler teeth and grating coupler at the 501nm.

In the final step enhancement factor and electric field intensity changes were calculated in terms of refractive index changes. Table 4.

Table **4** illustrate enhancement factor and electric field vs Refractive index

Refractive index	Enhancement factor	Electric field intensity
1.370	$4/20\times10^{13}$	۶۸۱۰۰۰۰
1.371	$4/19\times10^{13}$	6809200
1.372	$4/18\times10^{13}$	6808000
1.373	$4/17\times10^{13}$	6807700
1.374	$4/163\times10^{13}$	6803200
1.375	$4/16\times10^{13}$	6801540
1/38	$4/13\times10^{13}$	6790000
1/39	$4/08\times10^{13}$	6750000
1/40	$3/96\times10^{13}$	6700000
1/45	$3/29\times10^{13}$	6030000
1/50	$2/31+10^{13}$	5300000
1/51	$2/15+10^{13}$	5180000
1/52	$1/97+10^{13}$	5001000

This strong enhancement factor and relationship to refractive index can offer a system which can analysis single biomolecule with the high sensitivity [14].

III. CONCLUSION

A metallic nanoparticle and grating coupler structure is used as a nanoparticle-film coupling system. The FDTD simulation was used to calculate electric field distribution as well as enhancement factor.

In doing so two types of geometry was considered, that is nanorod and nanosphere. The materials for our simulation were gold and silver. Five different spacers (5, 10, 15, 20, and 25) along with s, p-polarization was chosen for the Ag-grating coupler.

Our result show that for nanoparticle-film coupling, the highest enhancement factor of (10^{13}) can be obtained for Ag nanosphere and Ag-grating coupler. This enhancement factor is due to the formation of double resonance system structure. Finally, our results illustrate the fact that our proposed system model can be used in single biomolecule detection.

REFERENCES

[1] M. Fleischmann, P.J. Hendra, and A. McQuillan, “Raman spectra of pyridine adsorbed at a silver electrode,” Chemical Physics Letters, vol. 26, pp.163-66, 1974.

[2] S. Cong, X. Liu, Y. Jiang, W. Zhang, and Z. Zhao " Surface Enhanced Raman Scattering Revealed by Interfacial Charge-Transfer Transitions," The Innovation, vol. 1, pp. 100051 (1-22), 2020

[3] M. M. Hernández, P. J. Rivero, J. Goicoechea and F. J. Arregui, “Trends in the Implementation of Advanced Plasmonic Materials in Optical Fiber Sensors (2010–

2020)," Chemosensors, vol. 9, pp. 64 (1-38), 2021.

[4] M. Choi, T. Kang, S. H. Choi and K. M. Byun, "Dual modal Plasmonic substrates based on a convective self-assembly technique for enhancement in SERS and LSPR detection," Optics Express, Vol. 29, pp. 6179-6187, 2021.

[5] C. Junfan, Z. Cong, Z. Jie, and Z. Yong, "Raman enhancement of large-area silver grating arrays based on self-assembled polystyrene microspheres," Optical Materials Express. Vol. 11, pp, 1234-1248, 2021

[6] B. Huang, J. Wang, S. Huo, and W. Cai, "Facile fabrication of silver nanoparticles on silicon for surface-enhanced infrared and Raman analysis," Surface and Interface Analysis, vol. 40, pp. 81-84, 2008.

[7] B. Messinger, K. Von Raben, R. Chang, and P. Barber, "Local fields at the surface of noble-metal microspheres," Physical Review B, vol. 24, pp. 649-657, 1981

[8] E. Le Ru, M. Meyer, E. Blackie, and P. Etchegoin, "Advanced aspects of electromagnetic SERS enhancement factors at a hot spot," Journal of Raman Spectroscopy, vol. 39, pp.1127-1134, 2008.

[9] P. Camargo, M. Rycenga, and Y. Xia, "Isolating and probing the hot spot formed between two silver nanocubes," Angewandte Chemie International Edition. Vol. 48, pp. 2180 (1-4), 2009

[10] K. Kneipp, H. Kneipp, and H. Bohr, "Single-molecule SERS spectroscopy," Surface-Enhanced Raman Scattering: Springer, vol. 60, pp. 261-277, 2006

[11] E. Le Ru and P. Etchegoin, "Rigorous justification of the|E|4 enhancement factor in surface enhanced Raman spectroscopy," chemical Physics letters, vol. 423, pp.63-66, 2006.

[12] Y. Hou, J. Xu, W. Li, and X. Wang, "Coupled sub wavelength gratings for surface-enhanced Raman spectroscopy," Physical Chemistry Chemical Physics, vol. 13, pp. 10946-109451, 2011.

[13] J. Camden, J. Dieringer, Y. Wang, D. Masiello, L. Marks, G. Schatz, and R. P. Van Duyne, "Probing the structure of single-molecule surface-enhanced Raman scattering hot spots," Journal of the American Chemical Society, vol. 130, pp. 12616 (1-7), 2008.

[14] K. Ma, J. M. Yuen, N. C. Shah, J. T. Walsh, J.r. M. R. Glucksberg and R. P. Van Duyne, "In Vivo, Transcutaneous Glucose Sensing Using Surface-Enhanced Spatially Offset Raman Spectroscopy: Multiple Rats, Improved Hypoglycemic Accuracy, Low Incident Power, and Continuous Monitoring for Greater than 17 Days" Anal. Chem. Vol. 83, pp. 9146–9152, 2011.

[15] E. Le Ru, E. Blackie, M. Meyer, P. Etchegoin, "Surface enhanced Raman scattering enhancement factors: a comprehensive study," The Journal of Physical Chemistry C, vol. 111, pp. 13794-13803, 2007.

[16] J. Gersten and A. Nitzan, "Electromagnetic theory of enhanced Raman scattering by molecules adsorbed on rough surfaces," The Journal of Chemical Physics, vol. 73, pp. 3023-3037, 1980.

[17] B. Sharma, R. Frontiera, A. Henry, E. Ringe, and R. Van Duyne, "SERS: materials, applications, and the future," Materials today, vol. 15, pp.16-25, 2012.

[18] A. Haes, C. Haynes, A. McFarland, G. Schatz, R. Van Duyne, and S. Zou, "Plasmonic materials for surface-enhanced sensing and spectroscopy," MRS bulletin, vol. 30, pp. 368-375, 2005.

[19] H. Wei, F. Hao, Y. Huang, W. Wang, P. Nordlander, and H. Xu, "Polarization dependence of surface-enhanced Raman scattering in gold nanoparticle− nanowire systems," Nano letters, vol. 8, pp. 2497-502, 2008.

[20] H. Xu and M. Käll, "Polarization-Dependent Surface-Enhanced Raman Spectroscopy of Isolated Silver Nanoaggregates," ChemPhysChem, vol. 4, pp. 1001-1005, 2003.

[21] Y. Zhou, X. Li, X. Ren, L. Yang, and J. Liu, "Designing and fabricating double resonance substrate with metallic nanoparticles–metallic grating coupling system for highly intensified surface-enhanced Raman spectroscopy," Analyst, vol. 139, pp. 4799-4805, 2014.

[22] Z. Yang, J. Aizpurua, and H. Xu, "Electromagnetic field enhancement in TERS configurations," Journal of Raman Spectroscopy, vol. 40, pp. 1343-1348, 2009.

[23] E. Hao and G. Schatz, "Electromagnetic fields around silver nanoparticles and dimers," The

Journal of chemical physics, vol. 120, pp. 357-66, 2004.

[24] J. Lee, J. Nam, K. Jeon, D. Lim, H. Kim, S. Kwon, H. Lee, and Y. D. Suh, "Tuning and maximizing the single-molecule surface-enhanced Raman scattering from DNA-tethered nanodumbbells," ACS nano, vol. 6, pp. 9574-9584, 2012.

[25] Z. Yang, Q. Li, F. Ruan, Z. Li, B. Ren, H. Xu, and Zh. Tian "FDTD for Plasmonics: Applications in enhanced Raman spectroscopy," Chinese Science Bulletin, vol. 55, pp. 2635-2642, 2010.

[26] P.B. Johnson and R. Christy, "Optical constants of the noble metals," Physical review B, vol. 6, pp. 4370 (1-10), 1972.

[27] T. L. McMeekin, M. L. Groves, and N. J. Hipp, "Refractive Indices of Amino Acids, Proteins, and Related Substances," Advances in Chemistry, Vol. 44, pp. 54-66, 1964.

[28] H. Zhao, P. H. Brown, and P. Schuck, "On the Distribution of Protein Refractive Index Increments," Biophysical Journal, Vol. 100, pp. 2309–2317, 2011.

[29] H. P. Erickson, "Size and Shape of Protein Molecules at the Nanometer Level Determined by Sedimentation, Gel Filtration, and Electron Microscopy," Biological Procedures Online, Vol. 11, pp. 32-51, 2009.

[30] X. Qian and S. Nie, "Single-molecule and single-nanoparticle SERS: from fundamental mechanisms to biomedical applications," Chemical Society Reviews, vol. 37, pp. 912-920, 2008.